Recent Innovations in Mechatronics (RIiM) Vol 8. (2021) No 1.
DOI: 10.17667/riim.2021.1/1.

Electric Vehicle Modeling and Simulation of Volkswagen Crafter with 2.0 TDI CR Diesel Engine

VW Vehicle 2020 Based PMSM Propulsion

Aminu BABANGIDA
Department of Mechatronics
Faculty of Engineering
University of Debrecen
Debrecen, Hungary
aminubabangida24@gmail.com

Péter Tamás SZEMES
Department of Mechatronics
Faculty of Engineering
University of Debrecen
Debrecen, Hungary
szemespeter@eng.unideb.hu

***Abstract*— The Internal Combustion Engine (ICE) used by conventional vehicles is one of the major causes of environmental global warming and air pollutions. However, the emission of toxic gases is harmful to the living. Electric propulsion has been developed in modern electric vehicles to replace the ICE.**

The research is aimed at using both Simulink and SIMSCAPE toolboxes in a MATLAB to model the vehicle. This research proposes a Volkswagen (VW) crafter with a 2.0 diesel TDI CR engine, manufactured in 2020. An electric power train, a rear-wheel driven, based on Permanent Magnet Synchronous Motor (PMSM) was designed to replace the front-wheel driven, diesel engine of the VW conventional vehicle.

In this research, a Nissan leaf battery of a nominal voltage of 360 V, 24 kWh capacity was modeled to serve as the energy source of the overall system. A New European Drive Cycle (NEDC) was used in this research. Other test input such as ramp was also used to test the vehicle under different road conditions. However, a Proportional Integral (PI) controller was developed to control both the speed of the vehicle and that of the synchronous motor. Different drive cycles were used to test the vehicle. The vehicle demonstrated good tracking capability with each type of test. In addition, this research found out that there is approximately about 19% more benefit in terms of fuel economy of electric vehicles than the conventional vehicles.

Keywords—MATLAB, NEDC, PMSM, PI, VW, ICE

I. INTRODUCTION

Environmental effects such as air pollutions and global warming are harmful to our health. The internal combustion engines (ICE) in our conventional automobiles are the major sources of such effects. “In recent decades, the research and development activities related to transportation have emphasized the development of high-efficiency, clean, and safe transportation”[1]. Electric vehicles have been developed nowadays to reduce these toxic effects and achieve safer transportation networks. In [2] Fuad Un-Noor et al stated that the development of electric vehicles is of immense benefit to our environment by reducing the adverse effect of greenhouse gas emissions. In their work, they reviewed various literature studies on Electric vehicles (EV’s) and have come up with the various design and development procedures right from vehicle modeling, EV configurations, battery management, and electrical machine drives. In electric vehicles (EV’s), the ICE propulsion has been replaced by electric propulsion, consisting of electric motor drives, energy sources, and other auxiliaries. Therefore, a reasonable effort has been made in the industrial automation in the transition from the traditional internal ICE vehicles to EV’s[3]. However, in a further study [4] Samir M. et al stated that “Greenhouse gas emission, fast depletion of fossil fuels, the oil crisis and the increased cost of petroleum products are the major factors that need a shift from internal combustion engines to Electric Vehicles”. Electric vehicles are solutions to this problem [5]. This research proposed a Volkswagen crafter with a 2.0 diesel TDI CR engine, manufactured in 2020. This paper focused on replacing the internal combustion engine of the proposed vehicle with electric motor propulsion in the rear wheel.

Reviewed literature has shown that many have worked on electric vehicles such as Wahono et al. in [6] compared three forms of range-extended engines for electric vehicles based on simulators. The study in [6] was done to overcome some disadvantages (such as its weight) of EV’s over the conventional Internal Combustion Engines vehicles. A further study in [7] by Marmaras Charalampos et al. simulated EV driver behavior in both road transport and electric power networks. The electric vehicle was modeled to investigate its integration in both the electric power system and transport systems of the road. In their studies, a multi-agent platform was used to model the driver behavior. However, they take a fleet of 1000 EV agents as case studies where aware and unaware profiles were chosen to explore the results. In conclusion, they discovered that the electric vehicle agent has both direct and indirect implications on road transport and electric power networks. In another study [8] presented a “ride comfort performance evaluation on EV conversion via

simulations". The study was aimed to investigate the vehicle ride comfort before it was converted to an electric vehicle. A full car model with 7 DOF was considered. Both the two results were validated by considering the vehicle performance before and after the transition from the conventional internal combustion engine form to an electric version one.

II. ELECTRIC POWER TRAIN

Electric power train for a Battery Electric Vehicle (BEV) consists of two parts: The electrical part and the mechanical part respectively. Figure 1 depicts the schematic of the general layout of the electric power train for BEV where M is the electric motor and the thin line represents the electrical part while the thick line is the mechanical part.

A. ELECTRICAL PART

The electrical part consists of the battery, the DC-DC convert, the inverter, the electrical machines, and the controller, which depends on the type of electrical machine used for the EV applications.

B. MECHANICAL PART

The mechanical part of the electric power train consists of the transmission system, the axles, the wheels, and the vehicle body. In this paper, the three-phase PMSM is abstracted into a simplified energy equivalent PMSM model that uses the losses obtained from the detailed PMSM model.

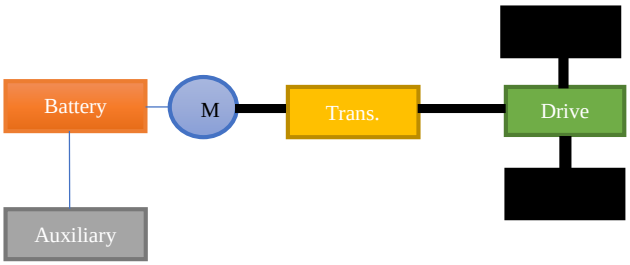

Figure 1: Battery Electric Vechicle

III. SIMULATION OF THE ELECTRIC POWER TRAIN DYNAMIC SYSTEM

Figure 2 is the simplified closed loop representation of the electric power train used in this paper for our electric crafter (e crafter) application. It consists of the Nissan leaf battery, the PMSM drives subsystem, the transmission subsystem, and the vehicle body subsystem. Method adopted [18] and [19].

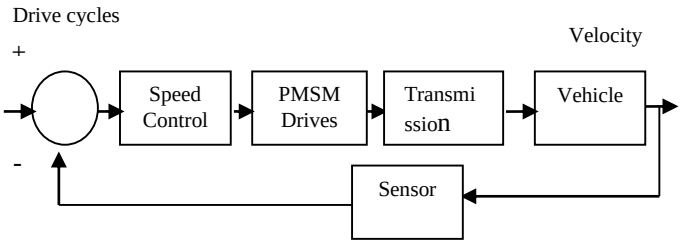

Figure 2: Simplified EV Power Train

A. Nissan Leaf Battery

In this research, a Nissan Leaf Battery of 2011 was used to design the electric vehicle. The battery has a nominal voltage of 360 V and a capacity of 24 kWh [9]. It consists of 48 modules, 4 cells (2 in parallel, 2 in series), making a total of 192 cells [10]. The total voltage of the battery pack is "2*4*48 = 403.2 V". Generally, the possible arrangement of the cells in a battery pack is studied by A. Emadi in [9].

TABLE I. *BATTERY SPECIFICATION*

Parameters	*Specifications*
Battery Nominal Voltage	360 V
Battery Capacity	24 kWh
Battery Charge	66.2 Ah
Energy Density	140 Wh/kg
Power Density	2.5 kW/kg
Battery Power	90 kW

B. PMSM Drives

A PMSM Motor is proposed in this research. A PMSM is widely used to overcome the disadvantages of a Brushless DC Motor (BLDC) [10]. P. Virani et al in [10] employed Field Oriented Control (FOC) approach to control the speed and the torque of the PMSM Motor for an electric vehicle application. Moreover, Espina et al in their study of Speed Anti-Windup PI strategies review for Field Oriented Control of Permanent Magnet Synchronous Machines, emphasized that Permanent Magnet Synchronous Machines (PMSM) are gaining market when compared to other AC Machines due to its higher efficiency, lower inertia, weight reduction and volume [11].

In this paper, the three-phase detail model of the PMSM designed was abstracted into an equivalent energy model that uses losses obtained by doing several numbers of experiments from our three-phase PMSM detail model.

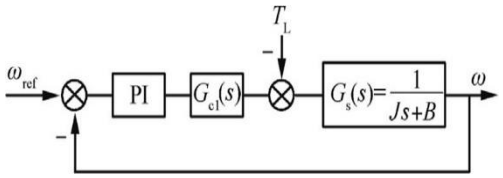

Figure 3: Simplified Three-PMSM Model [12]

$G_{cl}.(s)$ in the simplified PMSM closed–loop diagram represents the three-phase PMSM [12], the converter, dead time and PMSM current loop [12]. T_L represents the load torque of the motor, which is 360 Nm in our case, and ω is the speed to be controlled while ω_r is the reference speed which is 4250 rpm in this paper. Then the plant in the speed loop can be assumed as a first-order system with the time constant J/B, where J is the total inertia of PMSM, and B is the friction [12]. The PI controller can be represented mathematically as follows:

$$u(t) = k_p\, e(t) + k_i \int e(t)dt \qquad (1)$$

where k_p and k_i are the proportional and the integral coefficients, respectively; $e(t)$ is the error between the reference and the feedback signal [12].

TABLE II. *MOTOR SPECIFICATION*

Parameters	*Specifications*
Maximum Power	80 kW
Maximum Torque	280 Nm
Time Constant	0.02 s
Series Resistance	0
Rotor Inertia	3.90e-4 kgm^2
Rotor Damping	1e-5 Nm/(rad/s)

C. Vehicle Transmission System

A single-speed transmission system consists of various elements such as the gearbox, the torque converter, and the final drive. The function of each element as described in [1] is that the torque converter couples gearbox to the vehicle, the gearbox contains the appropriate gear ratios.

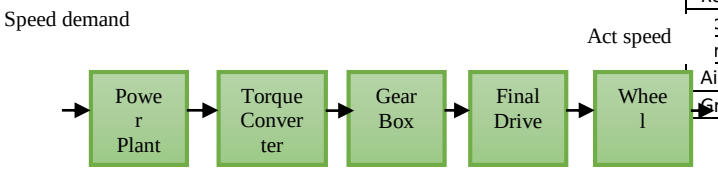

Figure 4: Transmission System

D. Vehicle Dynamics for Tractive Force Analysis

Vehicle dynamics is the study of the behavior of our vehicles in motion. It is studied under three categories such as longitudinal, lateral, and vertical dynamics. In this thesis, a Longitudinal dynamic of the vehicle is modeled in a MATLAB/SIMSCAPE/Simulink environment. "In practical terms, a vehicle not only travels on a level road but also up and down the slope of a roadway as well as around corners"[13].

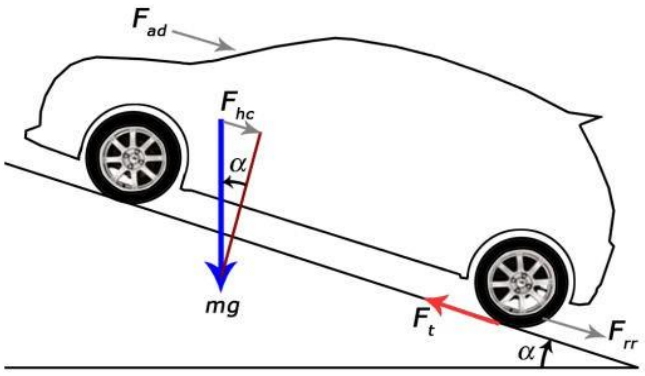

Figure 5: Vehicle dynamics [3]

The tractive force acting on the vehicle body can be described as in [3] and [14] as follows:

$$F_t = F_{ad} + F_{rr} + F_{hc} + F_A \quad (2)$$

Where F_{ad} is the wind resistance which is depends on the air density ρ, vehicle's front area A_f, drag coefficient C_d, and the vehicle's speed V, which is given by the formula:

$$F_{ad} = 0.5.\rho.C_d.A_f.V^2 \quad (3)$$

F_{rr} which is the rolling resistance which is depending on the vehicle weight w ($w = m * g$), rolling resistance coefficient C_{rr}, and the angle of inclination α.

$$F_{rr} = w.C_{rr}.cos\alpha \quad (4)$$

Grade and acceleration resistance forces are given as follows:

$$F_{hc} = w.sin\alpha \quad (5)$$

$$F_A = 1.04.m.a \quad (6)$$

Where m is the vehicle's mass in kg and 1.04 is the vehicle inertia, a is the vehicle's acceleration

And the tractive power and energy needed to propel the vehicle are given by the equations:

$$P = F.V \quad (7)$$

$$E = P.t \quad (8)$$

Where F is the tractive force in Newton and t is the time in seconds

TABLE III. *VEHICLE SPECIFICATION*

Parameters	*Specifications*
Vehicle Mass	3500 kg
Centre of Gravity	0.254 m
Front Axle	1.000 m
Rear Axle	1.346 m
olling Resistance	0.013 ohm
rag Coefficient	0.3
Air Density	1.225 kg/m^3
Gravity	9.81 m/s^2

E. Tire Dynamics Using Magic Formula

"The Tire-Road Interaction (Magic Formula) block models the longitudinal forces at the tire-road contact patch using the Magic Formula of Pacejka" [20]. In this paper, we used tires both in the front and rear axles of the vehicle model using magic formula. The tire coefficients are B, C, D, and E. The values of the coefficient as adopted from [20] are shown in Table IV.

TABLE IV. *TIRE SPECIFICATIONS [20]*

Surfaces	*Constant Coefficients*			
	B	C	D	E
Dry Tarmac	10	1.9	1	0.97
Wet Tarmac	12	2.3	0.82	1
Snow	5	2	0.3	1
Ice	4	2	0.1	1

F. Speed Controller

To control the speed of the PMSM, a PI controller was developed to control both the speeds of our motor and the vehicle. This PI controller was implemented in the energy equivalent model of our PMSM. PID controllers are used in many industrial applications due to their simple structure and robustness as well [15]. Due to the measurement noise, the derivative part is not normally used [15]. The Figure 6 below represents the general representation of the PI controller.

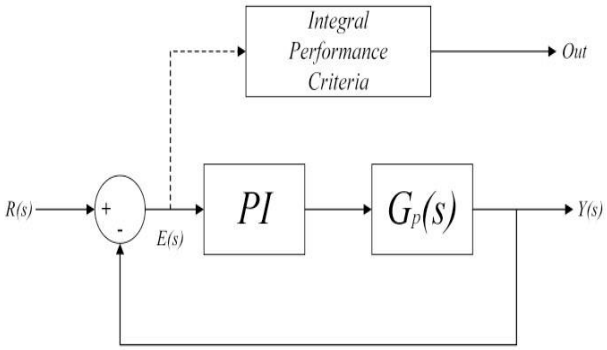

Figure 6. PI Controller [15]

G. Integral Performance Criteria

"Criteria based on disturbance rejection and system robustness are proposed to assess the performance of PID controllers" [16]. "The robustness is measured by a two-block structured singular value, and the disturbance rejection

is measured by the minimum singular value of the integral gain matrix" [16]. In this paper, we employ five criteria to assess the performance of our PI controller. these criteria are used in a closed-loop control system. The criteria are normally for different setpoints such as step input, ramp input, etc. In this research, the performance of our controller was assessed using the various inputs we used in this thesis. "It is well-known that a well-designed control system should meet the disturbance attenuation, setpoint tracking, robust stability, and/or robust performance" [16]. "The first two requirements are traditionally referred to as 'performance' and the third, 'robustness' of a control system" [16]. The following are the criteria stated in [16]:

$$IAE = \int_0^\infty |e(t)|.dt \quad (9)$$

$$ITAE = \int_0^\infty t.|e(t)|.dt \quad (10)$$

$$ISE = \int_0^\infty e(t)^2.dt \quad (11)$$

$$ITSE = \int_0^\infty t.e(t)^2.dt \quad (12)$$

Where IAE is the integral absolute error, ITAE is the integral time absolute error, ISE is the integral square error, and ITSE is the integral time squared absolute error [16]. We used these performance indexes in tunning our PID controller in this paper.

IV. MATLAB MODEL

Figure 7 is the complete model of our electric vehicle simulated in a Simulink environment. The model consists of the Nissan leaf battery, the PMSM drives, the transmission systems, and the vehicle subsystems.

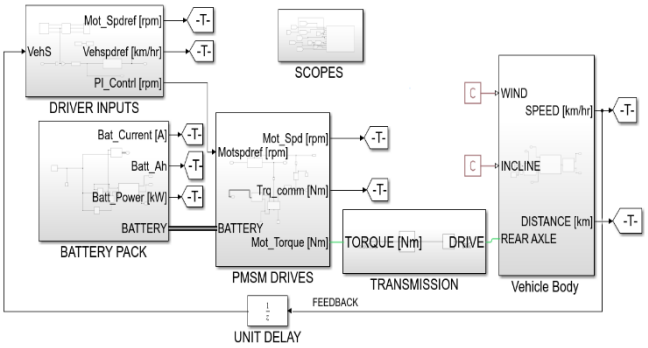

Figure 7: EV Simulink Model

V. RESULTS

Figure 8 below is the New European Drive Cycle (NEDC) used in this research to test our vehicle, other drive cycles were tested to comply with energy consumption and the rate of reduced emissions. In this paper, we used only three cycles at 200 seconds for the NEDC. Other drive cycles such as UDDS etc. were used to test our electric vehicle.

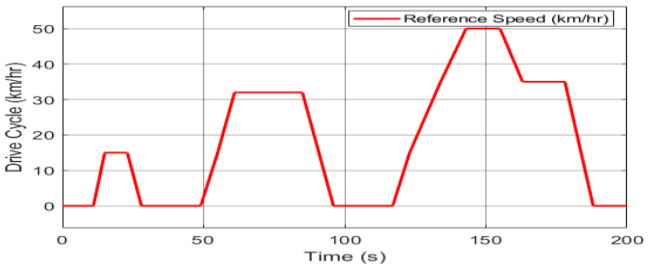

Figure 8: NEDC Drive Cycle

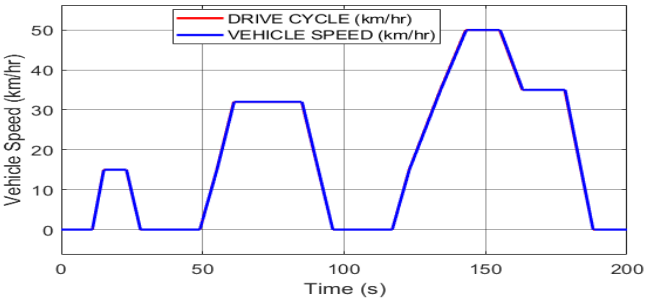

Figure 9: Vehicle Speed

While the figure 9 represents the both the reference speed and the vehicle achieved speed in 200 seconds.

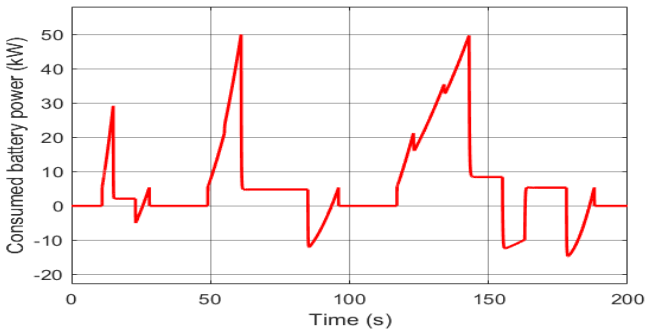

Figure 10: Battery Consumed Power

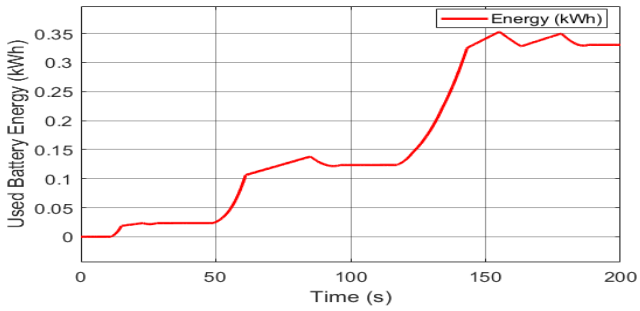

Figure 11: Battery Consumed Energy

Figure 10 is the battery consumed power in kilowatts. The Nissan leaf can give a power of over 90 kW out of which 50 kW was used for our electric vehicle. While figure 11 represents the energy used in kWh.

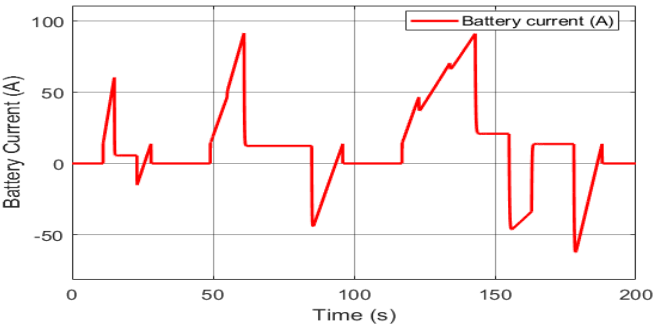

Figure 12: Battery Current

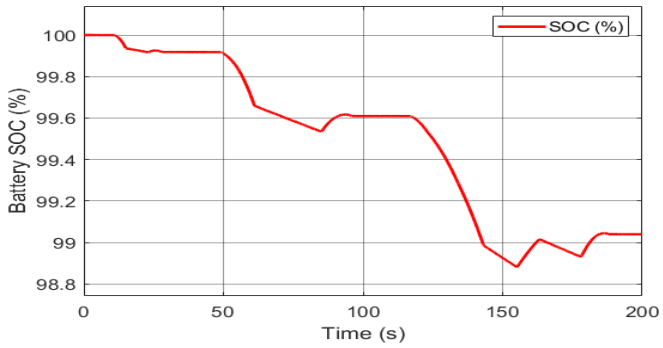

Figure 13: Battery SOC

Figure 12 represents the battery current. The battery draws a maximum current of 90 A when the vehicle is accelerating and a minimum current of – 60 A when decelerating. While figure 13 represents the battery state of charge (SOC) expressed in percentage which is approximately maintained at 99 % due to natural regenerative braking.

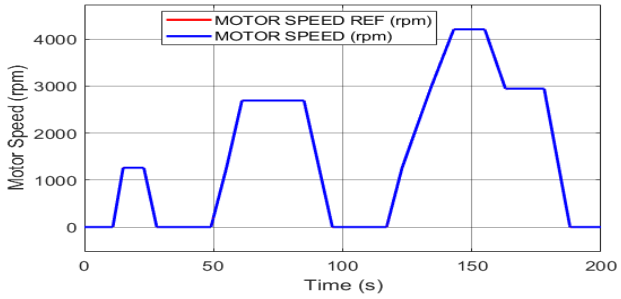

Figure 14: Motor Speed

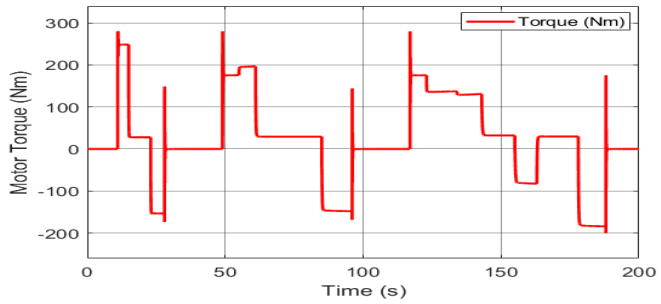

Figure 15: Motor Torque

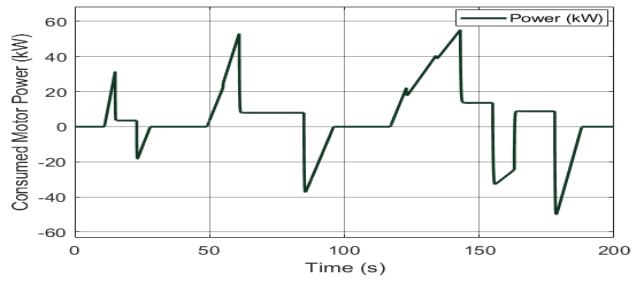

Figure 16: Motor Consumed Power

The motor reference speed was 4250 rpm and it subsequently tracks the actual speed successfully as shown in figure 14. Figure 15 is the maximum torque which is 280 Nm as seen in Table II of the motor specifications. While figure 16 represents the power consumed by the motor which is approximately 49 kW. We can analyze the losses in terms of the energy transmitted from the storage system which is the battery to the vehicle wheels. Figure 17 below plots both the energies consumed by the battery and the motor.

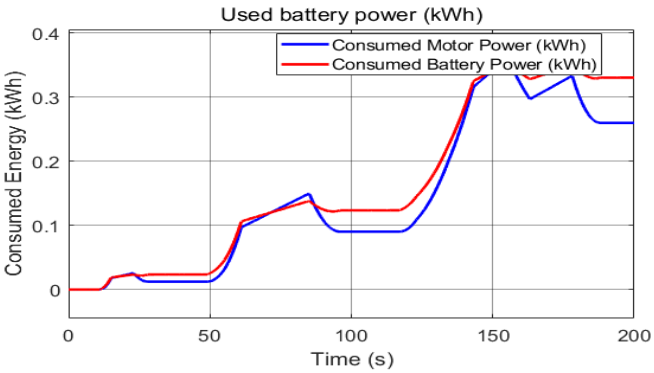

Figure 17: Consumed Energy in EV

The gap between the plots in figure 17 is the energy lost in transmitting from the energy supply system which is the battery to the motor which is our PMSM Motor.

It can be seen that:

If $E_b = 0.3305\ kWh$ is the energy consumed by our Nissan leaf battery,

$E_m = 0.2599\ kWh$ is the energy consumed by our PMSM Motor,

Then the energy efficiency, $\eta = \frac{E_m}{E_b} = 78.63\ \%$.

Therefore, this efficiency is much greater than the conventional vehicle with approximately 19 % efficiency. However, Duo Guanhao et al in [17] investigated that EV can reach up to approximately 15 % more efficient than conventional vehicles with ICE in terms of consumption rate (fuel economy). While figure 18 is the vehicle speed when tested by a ramp input. In this case, the vehicle accelerates from rest to a final speed of 5.55 m/s (20 km/hr).

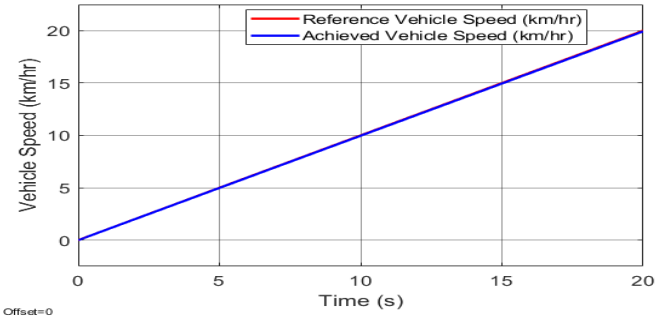

Figure 18: Vehicle speed due to Ramp input

A. PI Settings based on the Performance Matrix

The table below shows the PI controller setting based on the performance matrix obtained by taking several experiments until optimized gains have been achieved.

TABLE V: *PI CONTROL PARAMETERS*

Gains		*Performance Indices*			
K_p	K_i	*IAE*	*ISE*	*ITAE*	*ITSE*
152	153	2.4044	0.6088	15.6201	2.6532
154	154	2.4994	0.5489	17.9503	2.7353
153	153	2.4368	0.5850	16.0888	2.5714

VI CONCLUSION

This paper has presented the modeling and simulation of electric power train based PMSM Motor for a VW Crafter manufactured in the year 2020. A PI base classical control algorithm in the outer control loop of the PMSM was used to control both the speed of the vehicle and that of the motor.

REFERENCES

[1] G. Şenocak, *Modern Electric, Hybrid Electric, and Fuel Cell Vehilces*, Third edit. London Newyork: Tailor & Francis Group, an information business, 2019.

[2] F. Un-Noor, S. Padmanaban, L. Mihet-Popa, M. N. Mollah, and E. Hossain, "A comprehensive study of key electric vehicle (EV) components, technologies, challenges, impacts, and future direction of development," *Energies*, vol. 10, no. 8, pp. 1–82, 2017, doi: 10.3390/en10081217.

[3] T. A. T. Mohd, M. K. Hassan, and W. M. K. A. Aziz, "Mathematical modeling and simulation of an electric vehicle," *J. Mech. Eng. Sci.*, vol. 8, no. June, pp. 1312–1321, 2015, doi: 10.15282/jmes.8.2015.6.0128.

[4] S. M. Shariff, D. Iqbal, M. Saad Alam, and F. Ahmad, "A State of the Art Review of Electric Vehicle to Grid (V2G) technology," in *IOP Conference Series: Materials Science and Engineering*, 2019, vol. 561, no. 1, doi: 10.1088/1757-899X/561/1/012103.

[5] C. C. Cioroianu, D. G. Marinescu, A. Iorga, and A. R. Sibiceanu, "Simulation of an electric vehicle model on the new WLTC test cycle using AVL CRUISE software," in *IOP Conference Series: Materials Science and Engineering*, 2017, vol. 252, no. 1, doi: 10.1088/1757-899X/252/1/012060.

[6] B. Wahono, A. Nur, W. B. Santoso, and A. Praptijanto, "A comparison study of range-extended engines for electric vehicle based on vehicle simulator," *J. Mech. Eng. Sci.*, vol. 10, no. 1, pp. 1803–1816, 2016, doi: 10.15282/jmes.10.1.2016.5.0173.

[7] C. Marmaras, E. Xydas, and L. Cipcigan, "Simulation of electric vehicle driver behaviour in road transport and electric power networks," *Transp. Res. Part C Emerg. Technol.*, vol. 80, pp. 239–256, 2017, doi: 10.1016/j.trc.2017.05.004.

[8] S. A. Abu Bakar, M. F. Muhamad Said, and A. A. Aziz, "Ride comfort performance evaluations on electric vehicle conversion via simulations," *ARPN J. Eng. Appl. Sci.*, vol. 10, no. 17, pp. 7794–7798, 2015.

[9] A. Emadi, *Advanced Electric Drive Vehicles*.Ontario, Canada: Tailor & Francis Group, 2014.

[10] V. P. Virani, S. Arya, and J. . Baria, "Modelling and Control of PMSM Drive by Field Oriented Control For HEV," in *SSRN Electronic Journal*, 2019, pp. 1–11, doi: 10.2139/ssrn.3442515.

[11] J. Espina, A. Arias, J. Balcells, and C. Ortega, "Speed anti-windup PI strategies review for field oriented control of permanent magnet synchronous machines," in *CPE 2009 - 6th International Conference-Workshop - Compatability and Power Electronics*, 2009, no. June 2009, pp. 279–285, doi: 10.1109/CPE.2009.5156047.

[12] W. Lina, X. Kun, L. De Lillo, L. Empringham, and P. Wheeler, "PI controller relay auto-tuning using delay and phase margin in PMSM drives," *Chinese J. Aeronaut.*, vol. 27, no. 6, pp. 1527–1537, 2014, doi: 10.1016/j.cja.2014.10.019.

[13] S. Yang, Y. Lu, and S. Li, "An overview on vehicle dynamics," *Int. J. Dyn. Control*, vol. 1, no. 4, pp. 385–395, 2013, doi: 10.1007/s40435-013-0032-y.

[14] A. Saleem and A. Iqbal, "Calculation Along With Factors Affecting the Total Tractive Power and Energy Demand," 2020, pp. 0–4.

[15] T. Dogruer and N. Tan, "Design of PI Controller using Optimization Method in Fractional Order Control Systems," in *IFAC-PapersOnLine*, 2018, vol. 51, no. 4, pp. 841–846, doi: 10.1016/j.ifacol.2018.06.124.

[16] W. Tan, H. J. Marquez, and T. Chen, "Performance assessment of PID controllers," *Control Intell. Syst.*, vol. 32, no. 3, pp. 158–166, 2004, doi: 10.2316/journal.201.2004.3.201-1309.

[17] G. Du, S. Member, W. Cao, S. Member, and S. Hu, "Assessment of an Electric Vehicle Powertrain Model Based on Real-World Driving and Charging Cycles," vol. 9545, no. c, 2018, doi: 10.1109/TVT.2018.2884812.

[18] MathWorks Student Competition Team (2020). "Physical Modeling for Formula Student": Introduction to Simscape Retrieved October 18, 2020

[19] Isaac Ito, "Battery Electric Vehiclle Model in Simscape(htttps://githumb.com/mathworks/Simscape-Battery-Electric-Vehicle Model/releases/tag/1.0.0), GitHub, 2021.

[20] Pacejka, H. B. Tire and Vehicle Dynamics Elsevier Science, 2005.